

Dynamic angle measurement by means of a ring laser

To cite this article: Yu V Filatov *et al* 1997 *Metrologia* **34** 343

View the [article online](#) for updates and enhancements.

Related content

- [Precision angle measurement in a diffractive spectrometer by means of a ring laser](#)
- [Development of new methods and means of dynamic laser goniometry](#)
- [Development of precision laser goniometer systems](#)

Recent citations

- [A new method to eliminate the misalignment angle in dynamic goniometer based on fiber optic gyro](#)
Jiapeng Mou *et al*
- [Scale factor calibration and dynamic angle measurement method based on self-collimator and fiber optic gyroscope](#)
Jiapeng Mou *et al*
- [Design of a high-precision and non-contact dynamic angular displacement measurement with dual-Laser Doppler Vibrometers](#)
Lei Chen *et al*

Dynamic angle measurement by means of a ring laser

*Yu. V. Filatov, D. P. Loukianov
and R. Probst*

Abstract. A ring laser goniometer was investigated in different applications of precision angle measurement, such as the calibration of optical polygons and optical encoders, external angle measurement of rotating objects and inertial angle measurement by rotation of the goniometer itself. The results agree with standard methods of angle measurement to about $0,5 \mu\text{rad}$ ($0,1''$). Further improvement in accuracy is expected mainly from the reduction of noise in the mechanical and electrical setup of the measurement system.

1. Introduction

The laser with a ring cavity (ring laser) was suggested and developed soon after the conventional laser with a Fabry-Pérot cavity had been demonstrated. In the first paper devoted to the ring laser (RL), Rosental [1] analysed its distinguishing features and showed the possibility of using the RL for high-accuracy measurements of angular rate in relation to inertial space. As a result of these features, the RL served as a basis for laser gyro development. In the mid-1980s, after more than ten years of research and design work, the performance of the ring laser gyro had been enhanced to such an extent that it could be used as a sensor in inertial navigation systems in aircraft and other moving objects [2, 3].

On the other hand, it became clear at a very early stage of the RL development that it can be successfully used in angle-measuring techniques as a tool offering high resolution and accuracy over the full angular range of 360° . In a French patent [4], Catherin and Dessus first suggested a design of goniometer using the RL as a sensor. The implementation of the RL in a goniometer is similar to that of a circular scale in a conventional goniometer. Given the particular features of the RL, such a goniometer can be used for circular measurements in a dynamic mode of operation with high speed and accuracy and offers the possibility of automating the whole process of measurement. With the RL goniometer it is, for example, possible to carry out the calibration of a circular optical encoder with several thousand lines within a few seconds. The main metrological characteristic of the RL is that it offers

the advantage of a nearly perfect circular division as it is based on laser wavelength. It may therefore be used as an angle standard just as the linear laser is used as a length standard.

When the ring laser is used as a laser gyro in navigation systems, the lock-in effect can be avoided by using the so-called "dither" technique, i.e. by rotational oscillation of the RL. In the goniometer the RL is continuously rotated at a constant rate (so-called "rate-bias" technique) so that, in this case, the RL requires no additional means to avoid the lock-in effect. This mode of operation confers an important advantage on the use of the RL in a goniometer, because it allows the RL scale factor to be calibrated continuously against the angular reference of 360° .

The first example of an RL goniometer was constructed at the D. I. Mendeleyev Institute for Metrology (VNIIM, St Petersburg) by the authors of [5], to measure an optical polygon angle standard with an accuracy of about $2,5 \mu\text{rad}$ ($0,5''$). The first commercial RL goniometer was then produced by the Arsenal company in Kiev [6] in the early 1980s. This commercial system, GS-1L, is employed in the countries of the former Soviet Union and elsewhere, for example at the Slovakian Metrology Institute (SMÚ, Bratislava) [7], as a standard for the plane angle unit. Further development of the RL goniometer was carried out by some companies and universities [8, 9], particularly at the St Petersburg Electrotechnical University (SPEU) where such systems were developed, for example, for producing circular scales and for noncontact measurements of an object's angular position [10, 11]. The developments undertaken by the SPEU ultimately gave rise to the commercial laser goniometer system EUP-1L.

For the last three years, the SPEU has continued its activities in this field under the auspices of a joint project with the Flight Guidance Institute of

Yu. V. Filatov and D. P. Loukianov. St Petersburg Electrotechnical University, 197376 St Petersburg, Russian Federation.
R. Probst. Physikalisch-Technische Bundesanstalt, 38116 Braunschweig, Germany.

the German Aerospace Research Establishment (DLR), Braunschweig, and the Angles and Gears Laboratory of the Physikalisch-Technische Bundesanstalt (PTB) in Braunschweig. Initially, this project was supported by the German Federal Ministry for Research and Technology.

This paper presents some of the results of the research carried out under this project.

2. Principle of measurement

The principle of RL measurement is based on the frequency splitting between the two counterpropagating waves in the ring cavity caused by angular movements of the RL in its cavity plane [12]. This frequency, detected as frequency f of the RL's sinusoidal output signal, is proportional to the rotation rate or instantaneous angular velocity $\Omega = d\varphi/dt$ in the inertial space.

$$f = K(\Omega) \cdot \cos \theta \cdot \Omega, \quad (1)$$

where $K(\Omega)$ is the RL scale factor, a quantity which varies slowly with the rotation rate, and θ is the angle formed by the normal to the RL cavity plane (measuring axis) and the rotation axis. To a first-order approximation, K is

$$K \approx \frac{4 \cdot S}{\lambda \cdot L}, \quad (2)$$

where S and L are the RL area and perimeter and λ is the RL wavelength.

Integration of (1) over a time interval t yields

$$N_\varphi = K \cdot \cos \theta \cdot \varphi, \quad (3)$$

where N_φ is the number of periods of the RL output signal and φ is the angle of the RL rotation during the time of integration (it is assumed here that the dependence of K on Ω may be neglected). From (3) it follows that the angle of rotation φ is determined by the number of periods N_φ of the RL output signal together with K and $\cos \theta$.

$$\varphi = \frac{N_\varphi}{K \cdot \cos \theta}. \quad (4)$$

It follows from (4) that the RL scale factor K can easily be determined from the number of signal periods during one revolution $N_{2\pi} (\varphi = 2\pi)$.

$$K = \frac{N_{2\pi}}{2\pi \cdot \cos \theta}. \quad (5)$$

For the angle φ , (5) and (4) give the basic relation

$$\varphi = 2\pi (N_\varphi / N_{2\pi}). \quad (6)$$

For simplicity, we assume in the following $\cos \theta = 1$. From (4) we obtain the angle interval $\Delta\varphi_{RL}$ corresponding to one signal period of the RL which is

$$\Delta\varphi_{RL} = 1/K. \quad (7)$$

The principle of measurement of the RL goniometer is thus based on the integration of the RL output signal in angle measuring intervals. RL signal

generation can also be understood as a rotary scanning of a stationary circular standing wave. It thus provides a circular division with an increment of $\lambda/2$ [13]. This idealized interpretation best explains the potential of the RL to serve as a standard for circular and angular calibrations, as described below.

Figure 1 shows the principle of operation of the RL goniometer for the calibration of any type of angle converter. The goniometer includes the ring laser 1, the rotary platform 2, the spindle with drive 3, the angle converter consisting of the rotating part 4 and the non-moving part 5, indicating the angular positions of the rotary platform, and the counting unit 6. Devices 4 and 5 may, for example, take the form of an optical polygon together with an optical null indicator, or a circular encoder disc and its reading head.

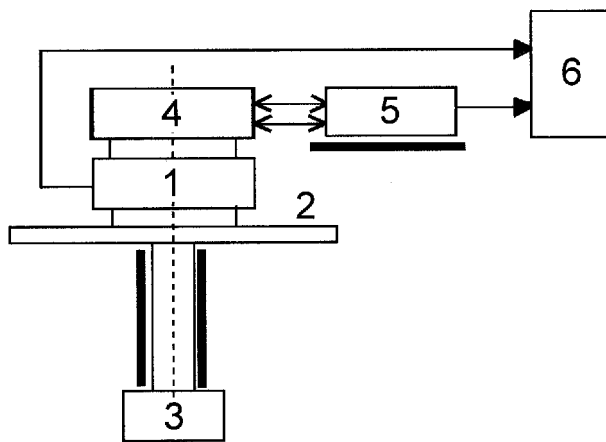


Figure 1. Schematic of the RL goniometer. 1 ring laser, 2 rotary platform, 3 spindle with drive, 4 rotating part and 5 non-moving part of angle converter, 6 counting unit.

Figure 2 shows the signal generation of the RL goniometer, where U_{RL} is the RL output signal and U_{AC} the angle converter output signal. The periods of the RL output signal are summed alternately by two counters, C1 and C2, within time intervals formed by the output pulses of the angle converter. So $N_{\varphi_i}^j$ is the

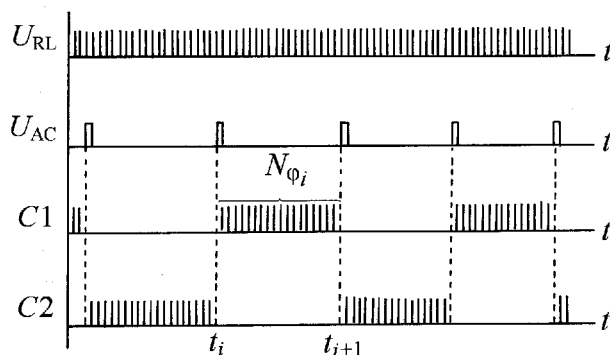


Figure 2. Schematic of the signal generation of the RL goniometer. U_{RL} ring laser output signal, U_{AC} angle converter output signal, $C1/C2$ counting results from the two counters.

result of summing over the i -th time interval between t_i and t_{i+1} , which, according to (3), yields

$$N_{\varphi_i}^j = \int_{t_i}^{t_{i+1}} f(t) \cdot dt, \quad (8)$$

where j is the number of revolutions of the platform from the beginning of the measurement.

The actual value of the scale factor K is derived according to (5) as the number of periods of the RL output signal during one revolution $N_{2\pi}$ divided by 2π . Considering that this number may change over time due to scale-factor drift, noise and other effects, it is useful to measure it as often as possible, preferably at every revolution. Also, the contribution of the Earth's rotation to the scale factor must be taken into account. This, however, can be kept constant with a sufficiently even rotation rate of the goniometer spindle or it can simply be corrected from a simultaneous measurement of time.

According to (6) and (8), the procedure of angle measurement during J revolutions of the platform may be written as

$$\varphi_i = \frac{2\pi}{J} \sum_j \frac{\int_{t_i}^{t_{i+1}} f(t) \cdot dt}{\sum_i^n \int_{t_i}^{t_{i+1}} f(t) \cdot dt}, \quad (9)$$

where n is the number of the angle converter intervals in 2π and the denominator terms of (9) represent the determination of the scale factor number $N_{2\pi}$ at every revolution.

Due to this continuous determination of the scale factor (so-called continuous self-calibration), the changes of the scale factor cause practically no measurement error. The main source of the random error is the angular vibration of the base of the measurement setup relative to the spindle. This may be explained by the fact that the RL is sensitive only to rotation in relation to inertial space, whereas the angle converter senses vibrations, which thus can contribute a measurement error. A systematic error component may also be caused by the influence of a magnetic field (for example, the Earth's magnetic field) on the RL, but this error usually does not exceed one microrad (several $0,01''$) [14]. When the angle converter is an optical polygon with a null indicator, the systematic component of the calibration error is related to the flatness error of the optical polygon faces and can amount to several microrad (several $0,1''$). Potential limits on the RL goniometer accuracy are set by random phase fluctuations of the RL output signal caused by quantum noise of the RL radiation. Theoretical and experimental estimates show that the limit of accuracy due to this influence is of the order of several tens of nanorad (several $0,001''$) [2, 15].

3. Instrumentation and measurement procedure

The results of the research considered in this paper were obtained using the RL goniometer system EUP-1L developed at the St Petersburg Electrotechnical University.

The EUP-1L allows angle calibrations to be carried out on both optical polygons and angle converters (for example, optical encoders) as described above. The EUP-1L system uses an RL with an He-Ne laser at $\lambda=633$ nm, a monolithic square cavity structure with four total reflecting prisms [16] (Figure 3), a perimeter of 44 cm and an angle interval $\Delta\varphi_{RL}$ of about $6,5 \mu\text{rad}$ ($1,3''$).

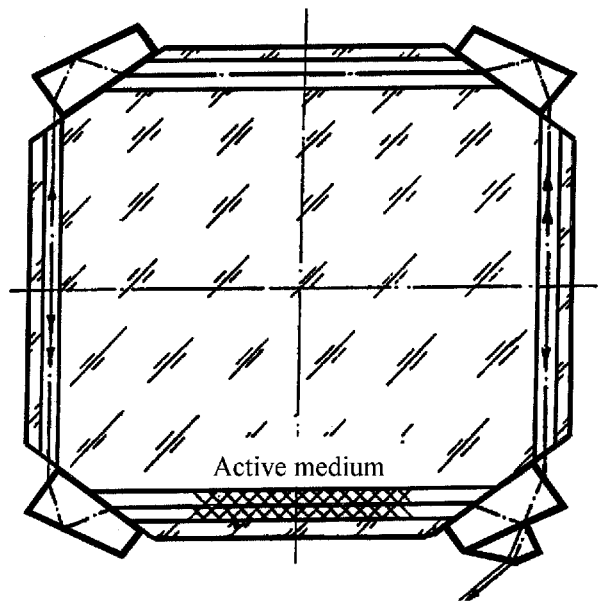


Figure 3. Optical design of the ring laser used in the EUP-1L goniometer. The 44 cm perimeter monolithic square cavity structure contains an He-Ne active medium, $\lambda=633$ nm. Four total reflecting prisms are mounted at the corners as well as one beam-combining prism for the signal generation (taken from [16]).

To increase the resolution, the RL output signal frequency was multiplied by a factor of 10 using a PLL circuit. The constant rotation rate of the RL goniometer spindle is approximately 0,7 rev/s. The spindle is carried in ball-bearings and driven by a dc motor via a belt drive. Slip-ring contacts are used to transmit the RL signal and the supply voltage. The size of the system is about 300 mm \times 300 mm \times 300 mm. Figure 4 shows the EUP-1L mounted on a PTB turntable. At the top of the instrument, an optical encoder is installed for reasons described below.

The system also has a function which makes it possible to measure an object's angular position by a noncontact method, as shown schematically in Figure 5. In operation, the EUP-1L depends on the rotation of the RL together with an optical polygon (OP). With this rotation, the light beam of a null indicator (NI) mounted



Figure 4. The RL goniometer EUP-1L mounted on a rotary table at the PTB. The RON 255 optical encoder may be seen at the top of the goniometer.

on the base of the system is scanned in a horizontal plane by its reflection from the faces of the rotating OP. The reference direction of the system is formed by the normal to a reference mirror (RM) which is fixed to the base. The NI generates pulses whenever the beam impinges normal to the RM and to the control mirror (CM) which is mounted on the rotatable object being measured. Consequently, the light beam reflection from each face of the OP leads the NI to give two output pulses (from the RM and the CM), and the interval between these pulses defines the angle formed by the RM and the CM. To measure this angle, the numbers N_φ of the RL output pulses given in the interval are counted. To obtain these numbers two counters (C1, C2) alternately sum the RL output pulses within the intervals, in a scheme similar to that shown in Figure 2. For the scale factor, it is also necessary to count the total number of pulses during one revolution $N_{2\pi}$. When these numbers are known, the angular position of the CM in relation to the position of the RM may be calculated using the formula

$$\varphi = 4\pi (N_\varphi / N_{2\pi}), \tag{10}$$

which is equivalent to (6) except for a factor of 2, which takes into account the doubling of the reflection angle at the OP. As this measurement of the angle φ is carried out on each OP face, the measurement is repeated with

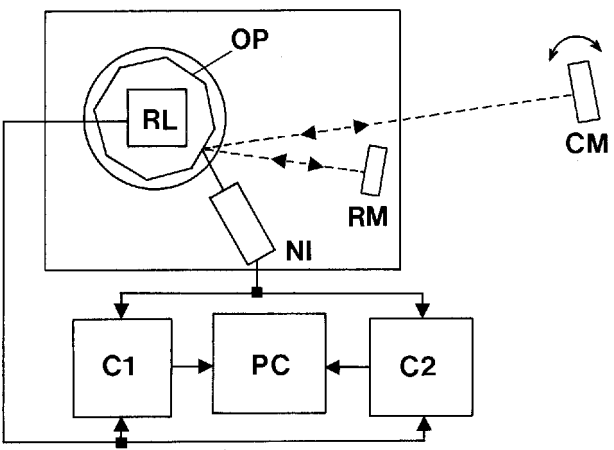


Figure 5. Principle of operation of the EUP-1L system for external angle measurements. OP optical polygon, RL ring laser, NI null indicator, RM reference mirror, CM control mirror, C1/C2 counters, PC personal computer.

the frequency $f = n/T$, where n is the number of the OP faces and T the time of one RL revolution.

The EUP-1L goniometer is connected to a personal computer which ensures data-processing using specific programs. For this investigation, two programs were used.

- (a) the “polygon” program, which allows angles between OP faces to be measured (OP calibration), and can also be used for calibrating angle converters such as optical encoders;
- (b) the “external angle” program, which was developed for the noncontact measurement of an object’s angular position (Figure 5).

Given the capabilities of the EUP-1L, the research was conducted in several directions as follows.

- calibration of optical polygons and comparison with the calibration methods of the PTB, using either an autocollimator or a phase-shifting interferometer. It was shown in [17] that these two methods can lead to slight differences between the results, caused by flatness errors of the OP faces.
- calibration of optical encoders. A commercial device, Heidenhain RON 255, was examined for this purpose. These measurements were aimed at obtaining an estimate for the repeatability and accuracy of the EUP-1L in this mode of operation.
- “external angle” measurements (Figure 5). In this mode of operation, we used a PTB angle-measuring turntable, the angular position of which was known with an accuracy of about $0,5 \mu\text{rad}$ ($0,1''$).
- use of the EUP-1L in the “inertial mode of operation”. In this application, because the RL acts as an inertial rotation sensor, EUP-1L directly measures angular displacements of the object on

which it is mounted (Figure 4 shows the EUP-1L mounted on a turntable for this purpose). This method of measurement offers the advantage that it is free from any need for external coupling or reference elements, and is independent of the location of the axis of rotation.

The turntable of the PTB used with the EUP-1L in the measurements described above, was mounted on a granite table in a laboratory at a controlled ambient temperature of $(20 \pm 0,1)^\circ\text{C}$. The turntable contains a high-precision air-bearing spindle with cylindrical and axial support. The spindle is rotated by a precise drive system which takes the form of a coarse friction wheel drive with a controlled dc motor and a piezo-electric fine-positioning drive. For angle measurement, the table is equipped with a Heidenhain RON 905 incremental rotary encoder system coupled inside the housing to the bottom of the spindle. The angular resolution of the encoder system, together with electronic interpolation, is about $0,17\ \mu\text{rad}$ ($0,035''$). The overall uncertainty of the system is $1\ \mu\text{rad}$ ($0,2''$) (coverage factor $k = 2$).

4. Results

4.1 Optical polygon calibration

For the investigation, a twelve-faced precision polygon of the PTB was used; this had been calibrated against an angle standard turntable together with an autocollimator and a phase-shifting interferometer [17]. The measurements with the EUP-1L were carried out using an interferential null indicator (NI) [18, 19]. This contained an incandescent lamp as light source and a photodiode as receiver.

The cross-section of the light beam, consisting of both beams of the NI interferometer, was a rectangle 20 mm in height and 16 mm in width. It should be noted that for the OP calibration at the PTB a light beam with a circular cross-section 25 mm in diameter was used.

The measurements with the EUP-1L were carried out by repeated RL counts over 50 to 100 revolutions of the goniometer rotary platform. The typical standard deviation for the mean values of these measurements was in the range $0,1\ \mu\text{rad}$ to $0,15\ \mu\text{rad}$ ($0,02''$ to $0,03''$). The main source of systematic error was found to be the inclination of the OP with respect to the rotation axis of the goniometer and the tilt of the NI with respect to its optical axis. We largely eliminated this influence by mounting the OP on a precisely adjustable device and obtained a coincidence with the rotation axis of about $25\ \mu\text{rad}$ ($5''$). The cross-calibration method [20] was used, so the whole measurement procedure consisted of twelve steps. In each step the OP was turned by 30° in relation to the rotary platform and measured again. The final results for the twelve polygon angles were then obtained from the well-known evaluation of 12×12 measurements.

Figure 6 shows the angular differences obtained from a comparison between the EUP-1L and the PTB methods using autocollimator (EUP.AC) and phase-shifting interferometer (EUP.PI). It may be seen that the differences from the interferometer data are smaller and do not exceed $\pm 0,75\ \mu\text{rad}$ ($\pm 0,15''$). It is assumed that the differences are due to the use of the interferential null indicator as well as the above-mentioned differences between the cross-sections of the light beams.

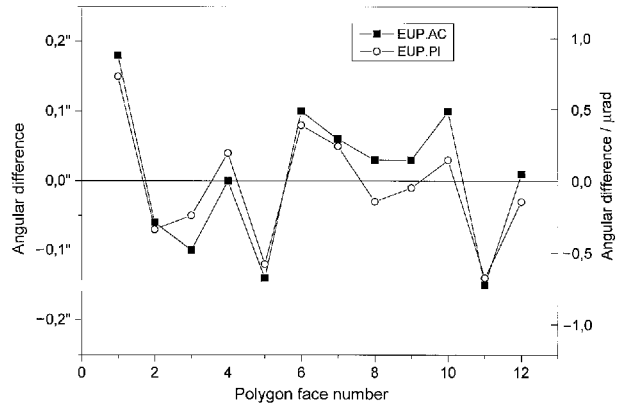


Figure 6. Differences between angle measurements on a twelve-faced optical polygon with EUP-1L and the PTB methods with autocollimator (EUP.AC) and phase-shifting interferometer (EUP.PI).

The EUP-1L measurements on optical polygons were also compared with measurements by the VNIIM. In this case, an eight-faced OP with faces $24\text{ mm} \times 56\text{ mm}$ in size was used. It should be noted that the flatness error of the faces of this OP was less than that of the twelve-faced OP of the PTB. The PTB OP had an average flatness error of about 11 nm (rms) on the square of the NI light beam cross-section, whereas that of the eight-faced OP was about 6 nm (rms) on the same square. Figure 7 shows the angular differences between the results obtained by the

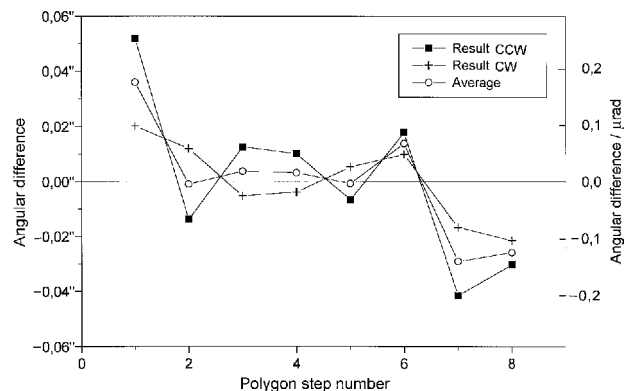


Figure 7. Differences between angle measurements on an eight-faced optical polygon with EUP-1L and the VNIIM autocollimator method for two directions of rotation of the EUP-1L rotary platform.

VNIIM and those obtained using the EUP-1L. The lines identified as CW and CCW in the figure correspond to results at different directions of rotation of the rotary platform of the EUP-1L. As may be seen, the angular difference does not exceed $\pm 0,17 \mu\text{rad}$ ($\pm 0,035''$) on average. It is assumed that these differences, which are much smaller than the data in Figure 6, are due mainly to the better flatness of the eight-faced OP.

As a result we can conclude that the error of optical polygon calibration by means of the EUP-1L is mainly dependent on the optical quality of the polygon faces, whereas the uncertainty of the calibration is $0,1 \mu\text{rad}$ to $0,15 \mu\text{rad}$ ($0,02''$ to $0,03''$) (type A evaluation) [22].

4.2 Optical encoder calibration

The measurements were carried out using the RON 255 optical encoder manufactured by Heidenhain. This device is an incremental angle encoder of medium accuracy with 18000 signal periods in 360° . The accumulated error for this encoder is specified within $25 \mu\text{rad}$ ($5''$). The RON 255 was mounted on the EUP-1L in coaxial direct coupling with the shaft of the goniometer spindle. The integral coupling device of the RON 255 allowed the influence of shaft wobbling and the non-coincidence of EUP- and RON-axes to be almost completely eliminated. Our electronic measuring system included a frequency divider for the encoder output signal, intended to reduce the number of angular intervals to be calibrated. The number of intervals defined by the division factor varied in the range from 30 to 360 (division factor 600 to 50).

As an example, some measurement results are presented with thirty encoder intervals. Twenty-five repeated measurements were performed, each covering twenty-five revolutions of the goniometer platform. Figure 8 shows the results of four measurements from this series.

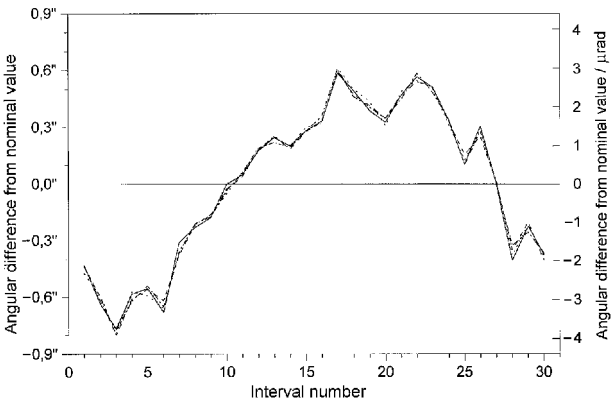


Figure 8. Results of the calibration of the RON 255 optical encoder. Values of thirty encoder intervals (each equal to 12°) from four repeated measurements.

It may be seen that the thirty encoder intervals deviate from their nominal angles of 12° by values

between $-4 \mu\text{rad}$ ($-0,8''$) and $+3 \mu\text{rad}$ ($+0,6''$), showing a typical first-harmonic distribution due to the encoder disc eccentricity. The measurement results were also processed with a view to obtaining the accumulated error of the encoder, i.e. the difference from the nominal value of an angle referred to an initial angle. Figure 9 shows the differences between the accumulated angles of the encoder and the mean values over all the measurements of the series, for the same four measurements as in Figure 8.

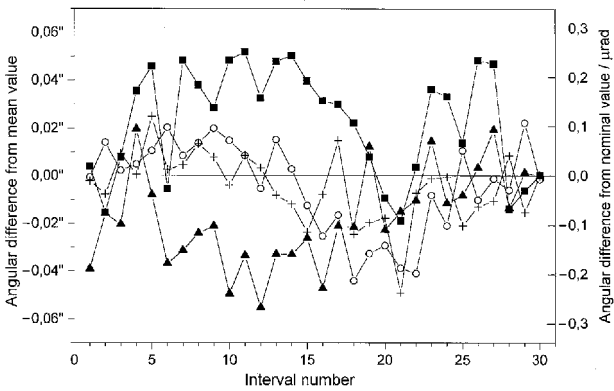


Figure 9. Difference between the accumulated angles of the thirty encoder intervals and their mean values, according to the results given in Figure 8.

The characteristics of these differences, which are within $\pm 0,3 \mu\text{rad}$ ($\pm 0,06''$), are partly of a random nature and partly of a systematic first-harmonic nature. The latter variation may be caused by the axial instabilities of the EUP-1L spindle or of the encoder bearing. The principal results of the optical encoder calibration series are summarized in Table 1. From these data it may be concluded that the type A uncertainty of the RL goniometer in this mode of calibration is about $0,1 \mu\text{rad}$ ($0,02''$) to $0,15 \mu\text{rad}$ ($0,03''$).

Table 1. Results of calibration of the optical encoder RON 255. The second and fourth rows represent the type A standard uncertainties evaluated from twenty-five repeated measurements.

Maximum deviation of thirty angle intervals from the nominal value	3,8 μrad ($0,78''$)
Average SD of thirty angle intervals from the mean values	0,092 μrad ($0,019''$)
Maximum deviation of thirty accumulated angles from the nominal values	13,0 μrad ($2,68''$)
Average SD of thirty accumulated angles from the mean values	0,12 μrad ($0,025''$)

4.3 External angle measurements

Making noncontact measurements of an external object's angular position (an object not connected to the measuring system in a mechanical way) is one of

the most interesting modes of operation of the EUP-1L system [10]. An important feature of this mode is an extremely wide angle-measuring range with a high accuracy. If the faces of the OP are rather wide (about 50 mm), this range $\Delta\varphi$ can be approximately defined by the formula

$$\Delta\varphi \approx 2 \arctan(D/L), \quad (11)$$

where D is the diameter of the CM whose angular position is measured (Figure 5) and L is the distance between the OP and the CM. If the distance is fairly small (about 0,2 m to 0,5 m), the measuring range $\Delta\varphi$ can extend up to a value of 30° . In this mode of operation, with the usual RL goniometer resolution of about $0,5 \mu\text{rad}$ ($0,1''$), the EUP-1L has a significant advantage over photoelectric autocollimators with their very small measuring range. It therefore was very important to carry out an investigation into this mode of operation using the PTB's precision standard turntable described above.

To avoid errors due to displacements of scanning beam caused by deviations from flatness of CM, the EUP-1L was mounted on the turntable and the control mirror was fixed to the granite plate at a distance of about 20 cm from the turntable. The EUP-1L was mounted so that the point of incidence of the NI beam on the OP face lay in the rotation axis of the turntable. In this way, the point of incidence of the beam on the CM surface is not displaced when the EUP-1L is rotated on the table.

Several series of measurements were carried out rotating the table with the EUP-1L by various angles. For each angle of rotation, a measurement was made over twenty-five revolutions of the goniometer platform. The type A uncertainty of each measurement, evaluated as the standard deviation of the mean over twenty-five revolutions of the platform, was about $0,25 \mu\text{rad}$ ($0,05''$) to $0,4 \mu\text{rad}$ ($0,08''$). Figure 10 shows a typical measurement result obtained when the turntable changed its position in an automatic run in

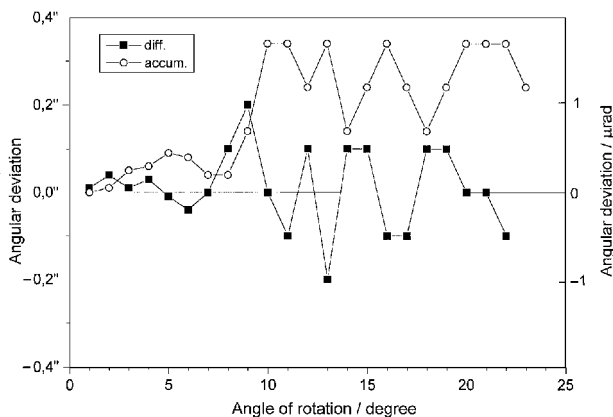


Figure 10. Step error (diff.) and accumulated error (accum.) of the EUP-1L in the external angle-measurement mode compared with the rotary table of the PTB over a range of 25° with 1° steps.

the range of 25° in steps of 1° . In the figure, the step error (diff.) and the accumulated error (accum.) of the measurements are given as deviations from the values indicated by the turntable. The data-processing program allowed an angular resolution of $0,05 \mu\text{rad}$ ($0,01''$) to be obtained only for angles within 10° , whereas for angles exceeding this limit, a resolution of only $0,5 \mu\text{rad}$ ($0,1''$) was obtained (cf. figure). It follows from the figure that the step measurement error is not greater than $1 \mu\text{rad}$ ($0,2''$) over the whole range of 25° and the accumulated error is within $1,7 \mu\text{rad}$ ($0,35''$) over the same range of angles.

4.4 Inertial angle measurements

A rate-bias RL in conjunction with an optical encoder was described as an instrument for inertial angle measurement with high resolution of angle and time [21]. We made the first tests of this method using the goniometer EUP-1L, equipped with the Heidenhain RON 255 optical encoder. The instrument was placed on the standard rotary table of the PTB as described above, which allows positioning with an angular accuracy of $0,5 \mu\text{rad}$ ($0,1''$) (Figure 4).

The principle of inertial angle measurement, as applied in this special case, is shown in Figure 11. First the ring laser scale factor is determined when the rotary table is in the rest position. This is done by counting the RL pulses during several revolutions of the goniometer spindle, using the 360° reference from the pulses of the optical encoder coupled to the spindle. Immediately after this calibration, the table rotates the goniometer through a certain angle and again comes to the rest position. The integral number of RL pulses counted during the rotation minus the stationary calibration value is a measure of the angle of rotation, as illustrated in Figure 11. The integral $\Sigma K(n)$ of the RL counts in the interval between the

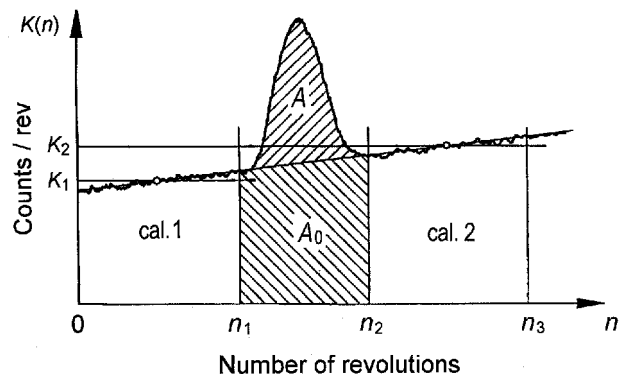


Figure 11. Principle of the RL goniometer inertial mode of operation. (0 to n_1) and (n_2 to n_3), calibration intervals; (n_1 to n_2), measurement interval; K_1 , K_2 , mean scale factors during calibration; $A_0 = (K_1 + K_2)(n_2 - n_1)/2$, interpolated stationary count integral during measurement; A , count integral during measurement minus A_0 , proportional to the inertial angle of rotation φ .

spindle revolutions n_1 and n_2 minus the interpolated stationary integral A_0 yields the integral A as a value proportional to the inertial angle of rotation φ . In the new rest position after the inertial measurement, another calibration of the scale factor can be carried out. If a linear drift of the scale factor between the first and second calibrations is assumed, the mean scale factor may be taken into account for subtraction during the measurement interval. In particular, if the calibrations performed before and after the measurement are taken over equal numbers of revolutions ($n_3 - n_2 = n_1$), the mean calibration values K_1 and K_2 can be used to calculate $A_0 = (K_1 + K_2)(n_2 - n_1)/2$, thus completely correcting a linear drift.

This principle shows that the stability of the RL scale factor and the linearity of its drift largely determine the accuracy which can be achieved in inertial measurements. In our measurements, the RL had been operated for a sufficiently long time under laboratory conditions that the scale factor usually had a relative drift of about 10^{-7} per hour and a random noise with a relative standard deviation of about $(1,5 \text{ to } 2,0) \times 10^{-7}$, which is, in units of angle, about $1 \mu\text{rad}$ ($0,2''$). It is worth noting that this scale-factor noise is not only due to the variation of the RL parameters but may be caused by variations of the optical encoder readout due to vibrations and lateral motions of the spindle axis.

We checked the inertial angle measurements using the EUP-1L in a series of repeated angular steps of 1° , 2° , 5° and 10° of the rotary table. The deviations of the inertial measurements from the reference values of the rotary table were evaluated (deviation = goniometer readout – reference value). The numbers of revolutions for the calibration and measurement intervals were selected according to the automatic run of the rotary table, and were maintained for all measurements of that series.

Figure 12 shows the results of four series of 1° measurements made in both directions of rotation. In all cases, the calibration times, in the range from 40 s to

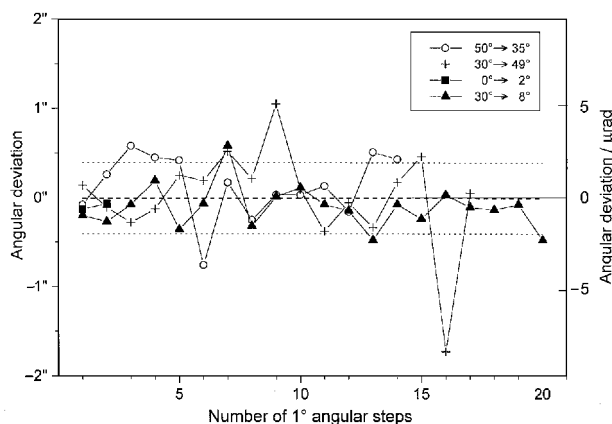


Figure 12. Angular deviations of the inertial measurements in comparison with those of the PTB rotary table, in four series of measurements of 1° steps in both directions of rotation.

90 s, were longer than the measurement times. Due to different speeds of rotation, these varied between 12 s and 30 s. The resulting angle deviations had a total mean value of $-0,05 \mu\text{rad}$ ($-0,01''$) and a standard deviation of $2 \mu\text{rad}$ ($0,40''$), as indicated in Figure 12 by dotted lines.

Other results obtained for 2° , 5° and 10° step measurements had a quality similar to that of the 1° measurements with slightly lower accuracy. For 2° we obtained a mean deviation of $0,5 \mu\text{rad}$ ($0,10''$) with a standard deviation of $2,2 \mu\text{rad}$ ($0,46''$), for 5° a mean deviation of $2,45 \mu\text{rad}$ ($0,51''$) with a standard deviation of $2,4 \mu\text{rad}$ ($0,50''$), and for 10° a mean deviation of $0,34 \mu\text{rad}$ ($0,07''$) with a standard deviation of $3,7 \mu\text{rad}$ ($0,77''$).

Let us consider potential sources of the uncertainties obtained. First there is a drift in the RL scale factor. As pointed out above, the relative drift of the scale factor was about 10^{-7} per hour. For the time interval of our measurements (usually not more than 100 s to 150 s, together with the calibration time), the uncertainty connected with the scale factor drift should therefore be about $0,5 \mu\text{rad}$ ($0,1''$) or less.

The second source of uncertainty is the scale-factor noise. This consists of noise from the readout variations of the optical encoder forming the counting interval and the random noise of the RL output signal. The noise from the former is not accumulated during the measurement. However, the integration of the RL noise during the inertial angle measurement gives rise to a random-walk uncertainty to be expressed as a standard deviation following a square-root law with time. This assumption was confirmed experimentally by repeated integrations of the RL signal in the stationary condition over different time intervals. The curve of the standard deviation σ obtained was fitted by the expression

$$\sigma^2 = [0,67^2 + 0,226^2 (t/s)] \mu\text{rad}^2$$

or, expressed in seconds of arc,

$$\sigma^2 = [0,14^2 + 0,047^2 (t/s)] (")^2.$$

The uncertainty of the inertial angle measurement due to the RL random noise was estimated on the basis of scale-factor data recorded over a long period. The recorded data were processed in accordance with the measurement procedure described earlier. Figure 13 shows the calculated mean standard deviation of the simulated measurements as a function of the measurement time in seconds, for calibration times of 30 s, 60 s and 80 s. The standard deviation increases as the square root of the measurement time, while the calibration time shows significant nonlinearity as the standard deviation decreases. The values are confirmed experimentally by the results of our inertial angle measurement. It is clear from these results that the uncertainty of this method depends significantly on the duration of the measurements, on the calibration and on the level of noise in the RL output signal.

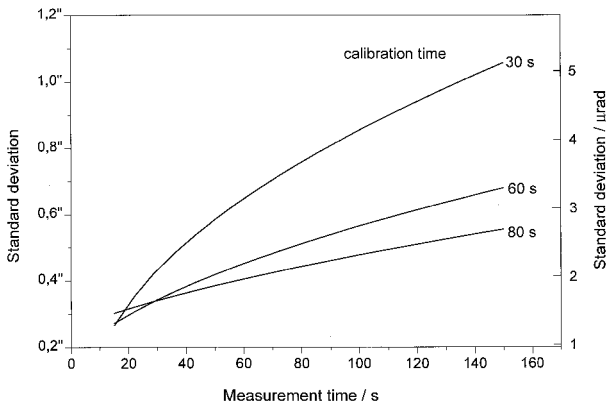


Figure 13. Estimated standard deviation of the inertial angle measurements obtained from a simulation of the measurement process on the basis of scale factor data recorded over an extended period.

5. Conclusions

Our investigations show that angle measurement by means of a ring laser goniometer is an effective and versatile method for applications such as calibration of optical polygons or optical encoders, external angle measurement of a rotating object or inertial angle measurement by goniometer rotation. The errors in these methods compared with standard angle measurements of the PTB are in the range $0.15 \mu\text{rad}$ to $1.0 \mu\text{rad}$ ($0.03''$ to $0.2''$). With the exception of the inertial method, where the uncertainty depends strongly on the time of measurement, the other applications described show values of uncertainty in the range $0.1 \mu\text{rad}$ to $0.4 \mu\text{rad}$ ($0.02''$ to $0.08''$). These uncertainties were generally evaluated from repeated measurements (type A evaluation). When compared with the standard methods of angle measurement the above values for the errors may therefore be regarded as partly type B uncertainties, which are mainly associated with specific influences of the optical and mechanical parts of the measurement setup (e.g. sensing of the polygon faces, shaft wobbling, etc.).

The quantum noise level of the ring laser has not yet been approached as the limit of accuracy. An improvement may be expected from the reduction of environmental disturbances such as vibration or temperature changes and optimization of the ring laser parameters, but also from the use of more precise mechanical components such as an air-bearing spindle with controlled direct drive, a high-accuracy optical encoder system as reference, and replacement of the slip-ring transmission of the RL signal by an optocoupler.

Acknowledgements. These investigations have been carried out within the framework of a joint BMFT project together with the Flight Guidance Institute, DLR Braunschweig. The authors would particularly

like to thank B. Stieler of the DLR for his initiative, support and continual interest, as well as R. Rodloff and other colleagues of the DLR for discussions. We also gratefully acknowledge the contributions of F. Posnien (DLR) and our co-workers M. N. Burnashev and P. A. Pavlov (SPEU) as well as those of A. Just and M. Krause (PTB). We also owe thanks to Yu. N. Shestopalov (VNIIM) for his contribution to the comparison of polygon calibrations.

References

1. Rosental A. H., *J. Opt. Soc. Am.*, 1962, **52**, 1143-1151.
2. Chow W. W., Gea-Banacloche J., Pedrotti L. M., Sanders V. E., Schleich W., Scully M. O., *Rev. Mod. Phys.*, 1985, **57**, 61-104.
3. Anderson R., Bilger H. R., Stedman G. E., *Am. J. Phys.*, 1994, **62**, 975-985.
4. Catherin J. M., Dessus B., French Patent No. 1511089; granted 26.01.68.
5. Blanter B. E., Filatov Yu. V., *Metrologiya (USSR)*, 1979, 3-9.
6. Vanyurikhin A. I., Zaitsev I. I., *Sov. J. Opt. Technol.*, 1982, **49**, 566-569.
7. Mokroš J., Vu K. X., *Jemná mechanika a optika*, 1993, **9**, 203-205.
8. Xu Y., Liao F., Dai R., Shen S., Situ Z., *Acta Metrologica Sinica*, 1985, **6**, 261-262.
9. Gelashvili N. V., Birkadze Sh. V., Kuryatov V. N., Orlov M. V., *Meas. Tech.*, 1988, **31**, 851-853.
10. Filatov Yu. V., Lukyanov D. P., Pavlov P. A., VDI Report No. 1118, 1994, 123-128.
11. Lukyanov D. P., Pavlov P. A., Filatov Yu. V., Symposium Gyro Technology, Stuttgart, 1991, 4.0-4.12.
12. Aronowitz F., In *Laser Applications* (Edited by M. Ross), New York, Academic Press, 1971, **1**, 133-200.
13. Schulz-DuBois E. O., *IEEE J. Quantum Electron.*, 1966, **2**, 299-305.
14. Krivtsov E. P., Filatov Yu. V., *Meas. Tech.*, 1989, **32**, 1140-1142.
15. Dorschner T. A., Haus H. A., Holz M., Smith I. W., Statz H., *IEEE J. Quantum. Electron.*, 1980, **16**, 1376-1379.
16. Zhuravleva E. N., Kuryatov V. N., Semenov B. N., 2nd Saint Petersburg Int. Conf. Gyroscopic Technology and Navigation, Part 2, St Petersburg, SCRI "Electropribor", 1995, 57-59.
17. Probst R., VDI Report No. 1118, 1994, 173-178.
18. Krivtsov E. P., Pavlov P. A., Filatov Yu. V., Yudin A. M., *Meas. Tech.*, 1986, **29**, 272-275.
19. Filatov Yu. V., *Sov. J. Opt. Technol.*, 1989, **56**, 204-207.
20. Sim P. J., In *Modern Techniques in Metrology* (Edited by P. L. Hewitt), Singapore, World Scientific, 1984, 102-121.
21. Rodloff R., Stieler B., Lübeck E., Wetzig V., Probst R., German Patent No. DE 42 31 935 C1, granted 7.4.94.
22. *Guide to the Expression of Uncertainty in Measurement*, Geneva, International Organization for Standardization, 1993.

Received on 10 February 1997.